Lead-Free Piezoelectric Ceramic in the $K_{1/2}Na_{1/2}NbO_3$-Solid Solution System

N. Marandian Hagh, E. Ashbahian, and A. Safari
Department of Ceramic and Materials Engineering
Rutgers, The State University of New Jersey
607 Taylor Road
Piscataway, NJ 08854-8065, USA

This article was submitted for publication in the IEEE-UFFC Transactions.

Abstract: Lead-based piezoelectric ceramics are only available materials for non-invasive medical ultrasound applications, while the embedded therapeutic and diagnostic procedures require lead-free piezoelectric transducer material. In order to achieve that, ultrasound material technology needs to be extended so as to be applicable for invasive ultrasonic applications. Along this goal, perovskite-type piezoelectric system of ($K_{1/2}Na_{1/2}NbO_3$-$LiTaO_3$-$LiSbO_3$; KNN-LT-LS) has been investigated. The effect of Ba^{2+} ion as an A-site additive has shown the improvement on the permittivity, piezoelectric charge coefficient as well as planar and longitudinal coupling coefficients. Piezoelectric charge coefficient, d_{33}, and longitudinal coupling coefficient, k_{33}, were shown up to 36% and 58% improvement upon 1 mol. % Ba^{2+} substitution. Remnant polarization increment along with coercive field decline was observed when 1 mol. % Ba^{2+} is introduced. This characteristic along with piezoelectric property improvement is indicating the soft piezoelectric behavior in this system. Microstructure studies have shown that substitution of 1 mol. %Ba^{2+} has lowered the grain size while improved the densification behavior of samples.

To demonstrate the performance capability of the base composition, a single element ultrasonic transducer was fabricated and the pulse-echo characteristics measured. At a center frequency of 3.56 MHz, the transducer had a -6 dB fractional bandwidth of 36.8% and an insertion loss of –8.36 dB. The studied lead-free piezoceramic system could be an excellent candidate for invasive and/or embedded medical ultrasound applications.

Keywords: *Lead-free piezoelectric materials, Ultrasonic transducers, Sodium potassium niobate ceramics*

I. INTRODUCTION

High electromechanical properties of the lead-based piezoelectric materials such as PZT [1, 2] have led to an extensive use of these materials in different piezoelectric applications. Even after losing some of their lead content during processing, PZT materials contain more than 60 weight percent lead. The lead loss occurs through vaporization at elevated temperature during sintering the ceramic to its final density. The practice of prohibiting its use in consumer products, sooner or later, will compel the US to follow Japan and the EU to impose exclusion of lead in transducer applications as well. Environmental and safety concerns with respect to the utilization, recycling, and disposal of Pb-based ferroelectric materials have induced a new surge in developing lead-free ferroelectrics, specifically those with properties comparable with their lead-based counterparts. Finally, the necessity for using transducers with lead-free materials in therapeutic and monitoring ultrasound devices which requires the embedded system in the body is another driving force for lead-free piezoelectric materials investigations.

In the past two decades, high frequency ultrasound imaging (HFUSI) has been the focus of many research studies to improve the image resolution to less than 10 μm. Such imaging modalities operate in the frequency range of 20-200 MHz. The immediate clinical applications of HFUSI are in the imaging of skin [1-3], anterior chamber of the eye [8, 9], gastrointestinal tract [2, 5] and the arterial walls [6, 7]. One of the main considerations for HFUS imaging modality is the design of a transducer with high sensitivity, SNR, and depth of penetration. These can be achieved by the use of a proper selection of piezoelectric material and low depth of focus utilizing synthetic aperture focusing technique and/or B/D-scanning modes [8]. Piezoelectric materials such as sol-gel lead zirconate titanate (PZT) [9], thin film spin coated polyvinylidene difluoride (PVDF) [10], Zinc oxide [11], lead titanate (PT) [12], and Lithium niobate (LiNbO3) [13] have already been explored and to some extent shown to be suitable for constructing transducers in this frequency range. The disadvantage of polymeric PVDF transducers is their poor sensitivity due to their low coupling coefficients and high dielectric loss, as shown in Table 1 [14]. Zinc oxide (ZnO) is a piezoelectric material with the highest piezoelectric properties among the tetrahedrally-bonded semiconductors. Its large piezoelectric coupling coefficients [15] have made it a technologically important and promising material in many applications, such as those characterized by surface acoustic waves. Table 1 shows the electromechanical properties of ZnO ceramics. Lead zirconate titanate (PZT) ceramic has extensively been used in piezoelectric transducers for a broad range of medical applications due to its excellent piezoelectric properties, see Table 1. As a result of its high dielectric constant, PZT ceramic must be well matched electrically to the coaxial line and pulser/receiver systems [16]. Therefore the application of PZT ceramic is limited to frequencies below 100 MHz [17] since it is almost impossible to electronically match the ceramic to any drive system.

Table 1. The electromechanical properties of some piezo-polymer and piezo-ceramics.

Property	PZT-5H	PVDF	ZnO	PT	PN
d_{33} (pC/N)	620	-20	12	68	100
K	4100	11	11.26	200	220
tan δ (%)	2.7	10		<2.0	6
k_t (%)	43	10	22.9	49	34
k_p (%)	65	-	46.6	6	-
Q_m	72	3-10		120	15
Z (MRayls)	33	4		35	20

d_{33}: the piezoelectric charge coefficient, k_t: the thickness coupling coefficient, k_p: the planar coupling coefficient, and K: dielectric constant.

Similar to morphotropic phase boundary (MPB) compositions observed in PZT ceramics, recent investigation has focused on the binary or ternary systems in non-lead based piezoceramics [1]. Among lead free piezoelectric materials, bismuth-layer structured ceramics such as $Sr_{x-1}Bi_{4-x}Ti_{2-x}Ta_xO_9$ are suitable candidates for sensors, resonators and filter applications due to their high T_c (>600ºC), anisotropic properties, and very high mechanical quality factor, Q_m (13500) [18-20].

Lately, ceramics with perovskite structures such as $Bi_{1/2}Na_{1/2}TiO_3$-based solid solution and alkaline niobate compounds $K_{1/2}Na_{1/2}NbO_3$ (KNN) have received considerable attention due to their higher piezoelectric properties and coupling coefficients than any other non-lead based piezoelectric ceramics [21-27] as shown in Table 2. KNN is a solid solution of $KNbO_3$ and $NaNbO_3$. Potassium niobate (KN) ceramic with ferroelectric orthorhombic symmetry at room temperature has the phase transitions similar to $BaTiO_3$ but with higher T_c (~420 ºC). $NaNbO_3$ (NN) ceramic is an orthorhombic anti-ferroelectric at room temperature with T_c = 355ºC [1, 28]. Therefore, the KNN system resembles the PZT system in the sense that it is comprised of ferroelectric and antiferroelectric end-members. The addition of KN to NN results in a ferroelectric phase with a high T_c exceeding 400ºC, and is accompanied by a decrease in critical electric field needed to induce a ferroelectric phase transition as compared to that of pure NN [22-27]. The minimum amount of K^+ needed in the NN host to induce a ferroelectric phase has been reported as 0.6 atomic percent, for which the spontaneous polarization is 33 μC/cm^2 [1]. Unmodified KNN ceramics are difficult to sinter, and exhibit poor aging in air. Samples that are synthesized via pressureless sintering are known to exhibit poor piezoelectric properties [29, 30]. Hot pressing or hot forging of KNN has proven to be very effective in obtaining improved piezoelectric properties as compared to those obtained otherwise [27,31]. Attempts have also been made to improve the sinterability and piezoelectric properties of KNN through A-site or B-site addition/substitutions [32-37]. Saito et al.'s pioneering work on MPB compositions in the binary KNN- $LiTaO_3$ system, or ternary KNN-LT-$LiSbO_3$ [38, 39] has explicitly shown that piezoelectric properties comparable to hard PZT-4 can indeed be achieved.

Table 2. Piezoelectric properties of various non-lead based piezoelectric ceramics.

Properties/Materials	BT[a]	SBTT3 (0.3)[b]	KNN-LT[c]	BiNT-BiKT-BT[d]	NBiT[e]	PZT-4[f]
$\varepsilon_{33}^T/\varepsilon_o$	1700	188	1256	1141	140	1300
Dielectric Loss, (%)	0.5	-	1.6	-	10 (at 400ºC)	0.4
k_{33}	0.5	0.128	-	0.56	0.15	0.7
k_p	0.36	0.04	0.51	0.33	-	0.58
d_{33} (pC/N)	190	14.6	230	191	18	289
Q_m	-	1243	-	84	100	-
T_c (ºC)	115	540	323	301	~600	328

a: BT: $BaTiO_3$ [46]
b: SBTT3(0.3): $Sr_{0.3}Bi_{3.7}Ti_{2.7}Ta_{0.3}O_{12}$ [47]
c: KNN-LT: $K_{0.5}Na_{0.5}NbO_3$-$LiTaO_3$ [48]
d: BiNT-BiKT-BT: $Bi_{0.5}Na_{0.5}TiO_3$-$Bi_{0.5}K_{0.5}TiO_3$-$BaTiO_3$ [23]
e: NBiT: $Na_{0.5}Bi_{4.5}Ti_4O_{15}$ [49]
f: PZT-4: A-site substituted hard PZT [46]

The purpose of this study is to investigate the effects of processing method and donor dopant on the dielectric, piezoelectric, electrical, and acoustic properties of the MPB composition in the KNN-LT-LS ternary system. For the processing methods, we study mixed oxide of initial base constituents in the ternary system. For the donor doping, we have chosen Ba^{2+} as an A-site substitution based on the ionic size considerations and valence so as to explore the possibility of imparting "soft" characteristics to the MPB composition in a way similar to what has been accomplished in the past for the PZT system. We also examine and report our preliminary results of transducers fabricated from such ferroelectric ceramics.

II. EXPERIMENTAL

The compositions of interest were synthesized according to the A-site defect formula $(A_{1-mx/n}D_x)BO_3$, where x is the mole fraction of dopant (x = 0.0, 0.5, 1.0, 1.5, 2.0), D denotes the dopant (Ba^{2+}), m and n are the valences of dopant and A-site ions respectively. Here A and B represent

the A-site and B-site cations in the KNN-LT-LS host, i.e. $((K_{0.5}Na_{0.5}Li_{0.04})_{1-2x}Ba_x(Nb_{0.86}Ta_{0.04}Sb_{0.06})O_3$.

Preparation of compositions with different molar percents of Ba^{2+} was carried out by wet ball milling of appropriate molar ratio of K_2CO_3 (Alfa Aesar, 99.0% min.), Na_2CO_3 (Alfa Aesar, 99.5% min.), Nb_2O_5 (H.C. Starck, 99.9%), Li_2CO_3 (Alfa Aesar, 99.0% min.), Ta_2O_5 (Alfa Aesar, 99.85% min.) and Sb_2O_5 (Alfa Aesar, 99.99% min.) for 12 hours using the ZrO_2 milling media in Aceton. The mixed powders were dried over night at 110ºC in an oven. Then the batches were pre-reacted at 850ºC for 5 hours. Samples that were 12mm diameter and 1 mm thickness were sintered at 1150ºC for one hour in an oxygen atmosphere. Qualitative X-ray phase analysis was carried out on Philips D500 with Cu K_α radiation using a step-scan of 0.03 degrees per step in 2θ and 2 seconds dwell time per step. The microstructures of the sintered samples were studied by field emission scanning electron microscopy (FESEM) LEO (ZEISS) 982. Grain size measurements were carried out using the mean intercept length method from at least five different areas of sample. The top and bottom surfaces of samples were lapped and then poled under an electric field intensity of 50kV/cm for 15 min in silicon oil at 100ºC. Piezoelectric charge coefficient, d_{33}, was directly recorded from a Berlincourt piezometer (Channel Products, Inc.). Permittivity and dielectric loss were measured at 1 kHz using the HP 4194A impedance/gain-phase analyzer. Piezoelectric planar and thickness coupling coefficients, (k_p and k_t) were calculated from the resonance and anti-resonance frequencies of the impedance traces, and in accordance to the IEEE Standards [40]. Longitudinal coupling coefficient, k_{33}, was estimated from the thickness and planar coupling factors. The room temperature polarization-field *(P-E)* hysteresis loops were measured with a Sawyer-Tower circuit that was operated at 50 Hz (Radiant Technologies Inc.). The resistivity-temperature measurements were carried out using a commercial I-V testing system (Radiant Technologies Inc.) in a silicon oil bath with controlled temperature.

III. RESULTS AND DISCUSSION

Fig. 1 compares the X-ray traces of the sintered samples with different molar percentages of Ba^{2+}. When the Ba^{+2} content is $\leq$ 1.0 mol%, the prepared samples were orthorhombic specified by the splitting of the (220) and (002) reflections and by higher intensity counts for the (220) peaks. Further increase in the Ba^{2+} beyond 1.0 mol% concentration reduces the splitting of (220) and (002) orthorhombic reflections. This indicates that the dopant is incorporated into the perovskite structure, and on the other hand forms a significant amount of tetragonal phase at 1.5 mol%, and transformed into a pseudo-cubic phase at 2.0 mol.% Ba^{+2}. The transformation of orthorhombic phase to pseudo-cubic state has also been reported for the addition of Ta dopant into KNN ceramics [35]. In the mean time, x-ray data up to 2 mol.% did not show any evidence of detectable second phase.

Fig. 2 shows SEM micrographs of unpolished top surfaces of the sintered samples with different Ba^{2+} concentrations. The grains of all prepared samples were cubic shape and a decrease in grain size was witnessed with increasing Ba^{2+} content. As shown in Fig. 3, the undoped composition had an average grain size of ~3 µm, while the grain size of samples with 2 mol% of Ba^{2+} was ~0.5 µm. It appears that Ba^{2+} is an effective grain growth inhibitor in this system.
Table 3 shows the effect of Ba^{+2} content on the physical and electromechanical properties of sintered ceramics. Fig. 3 also depicts the effect of Ba^{+2} substitutions on the relative density of sintered samples. The samples with 0.5 -1.0 and 2.0 mol% Ba^{2+} substitution had the highest and lowest relative densities, respectively. Interestingly the relative density of samples with 2.0 mol% Ba^{+2} was even much lower than those of samples made from undoped composition. This was attributed to the effect of Ba^{+2} on the increase of sintering temperature. No signs of liquid phase formation at the applied sintering temperature were observed. Similar observation was reported by Saito [39] for samples without Ba^{+2} whose relative densities and sintering temperature were 100% and 1150 °C, respectively. The sintering temperature range for the base composition with

full densification has been reported to be 50 °C in which melting occurs at 1175 °C while samples still retain their original shape.

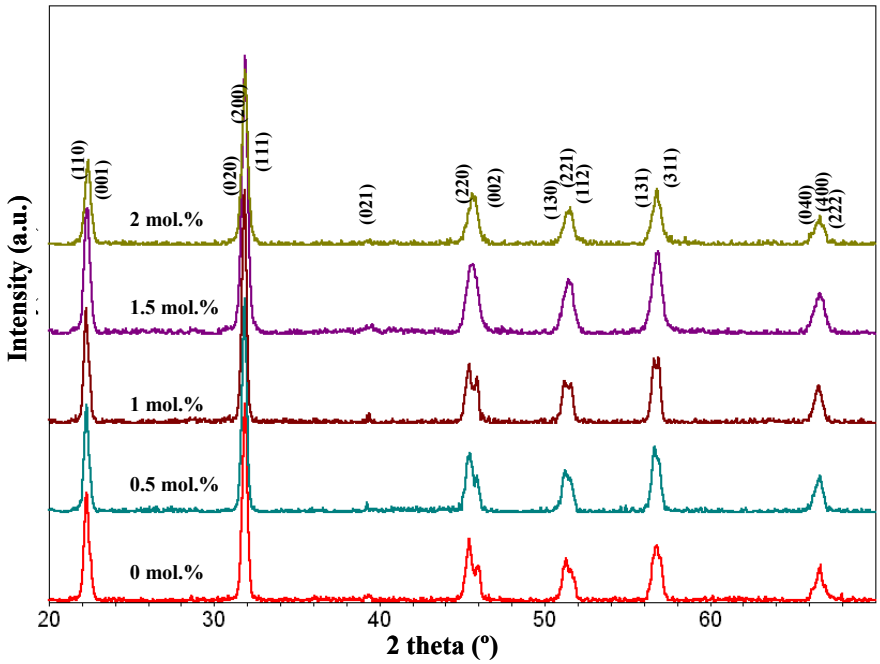

Fig. 1- The X-ray traces of the sintered samples with different molar percentages of Ba^{2+}.

.

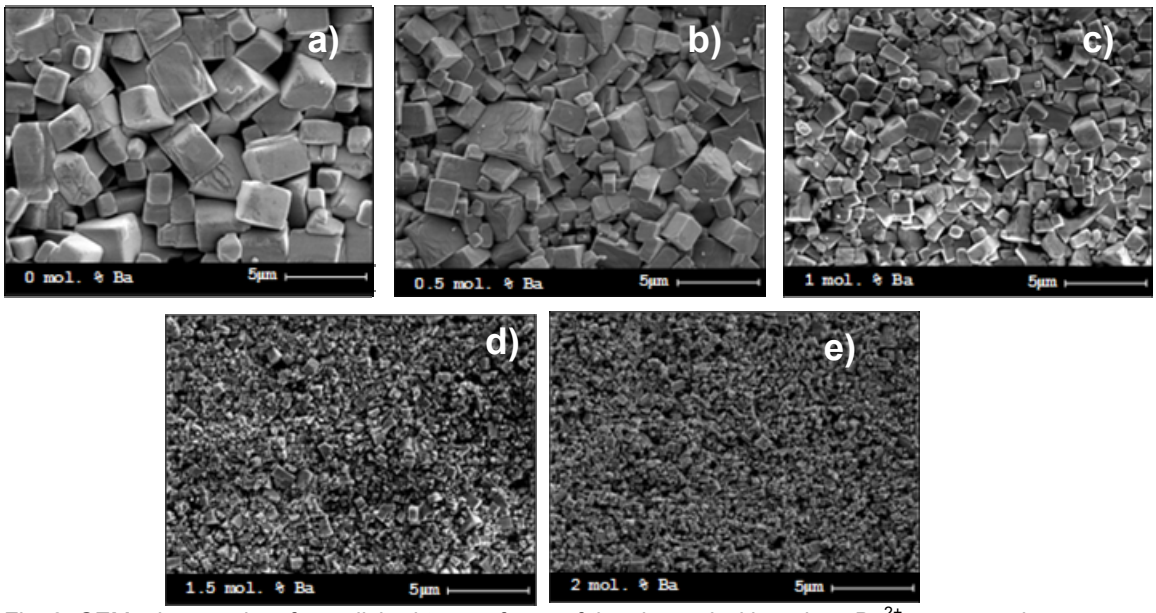

Fig. 2- SEM micrographs of unpolished top surfaces of the sintered with various Ba^{2+} concentration.

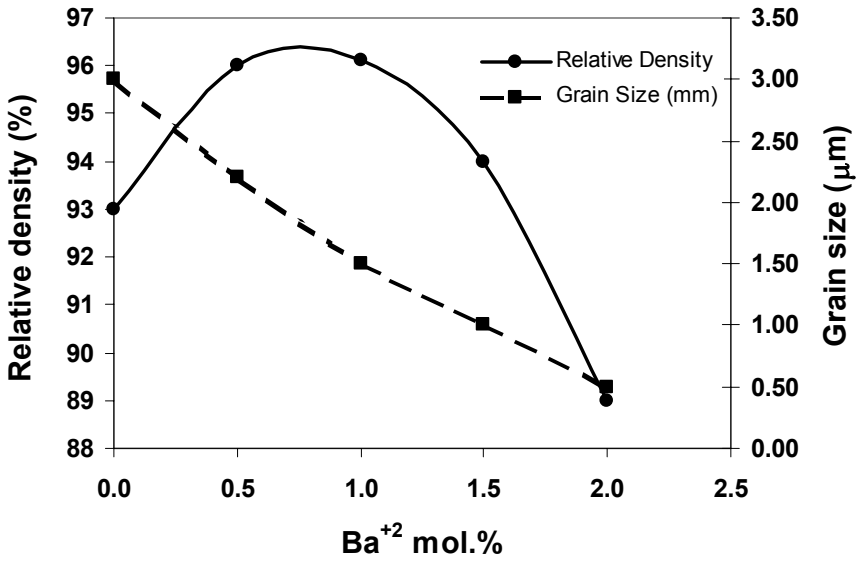

Fig. 3- The effect of Ba^{+2} substitution on relative density and grain size of the sintered samples in oxygen atmosphere at 1150 ºC-1hr.

Table 3. Physical and electromechanical properties of sintered ceramics with different mol. % of Ba^{+2}.

Properties	Mol. % Ba^{2+}				
	0.0	0.5	1.0	1.5	2.0
d_{33}, *(pC/N)*	154	165	210	71	45
g_{33}, $\times 10^{-3}$ *(Vm/N)*	26.2	24.1	20.2	7.3	5.5
K *(@ 1 kHz)*	664	773	1173	1104	917
tan δ *(@ 1 kHz)*	0.029	0.049	0.026	0.029	0.062
Poisson's ratio	0.345	0.410	0.380	0.360	0.325
Coupling Coefficients:					
k_p	0.222	0.279	0.348	0.177	0.104
k_t	0.284	0.244	0.369	0.270	0.141
k_{33}	0.355	0.364	0.491	0.320	0.175
k_{31}	0.127	0.152	0.194	0.101	0.061
Velocity (m/s)	5690	6134	5713	5990	5222
Z (MRayls)	25.89	28.77	26.85	27.56	22.72
Q_m:	85.4	65.5	72.0	43.0	69.1
Frequency Constant:					
N_p *(Planar)*	3197	3321	3191	3272	3073
N_t *(Thickness)*	2845	3067	2856	2995	2611
Relative Density, %	93.0	96.0	96.1	94.0	89.0
Curie Temperature, *(° C)*	298	281	266	208	190
Remnant Polarization *(μC/cm²)*	13.55	18.56	20.74	8.20	7.42
Coercive Field *(kV/cm)*	14.46	10.46	9.83	7.70	10.87

Fig. 4 illustrates the polarization-field behavior of samples with different molar percentages of Ba^{2+}. A well saturated hysteresis loops were obtained for the composition with $Ba^{+2} \leq 1.0$ mol.%. The remnant polarization (P_r) and coercive field (E_c) of the base composition (0.0 mol.% Ba^{+2}) were ~13.5 μC/cm^2 and ~14.5 KV/cm, respectively. The P_r values increased with increasing the Ba^{+2} concentration, reaching maximum value of ~21 μC/cm^2. Further increase of the Ba^{+2} concentration gave rise to unsaturated hysteresis loops and a significant decline of the polarization values. The P_r values at high mol.% Ba^{+2} were even smaller than that of the base composition, see also Table 2. The coercive field values of all samples doped with the Ba^{+2} were smaller than that of samples prepared with base composition. The decrease of the coercive field values illustrated that the addition of the Ba^{+2} transformed the base composition into a soft ferroelectric material. This action is similar to the addition of various dopants to the PZT ceramic with morphotropic phase boundary composition for transforming it to what is know as soft PZT

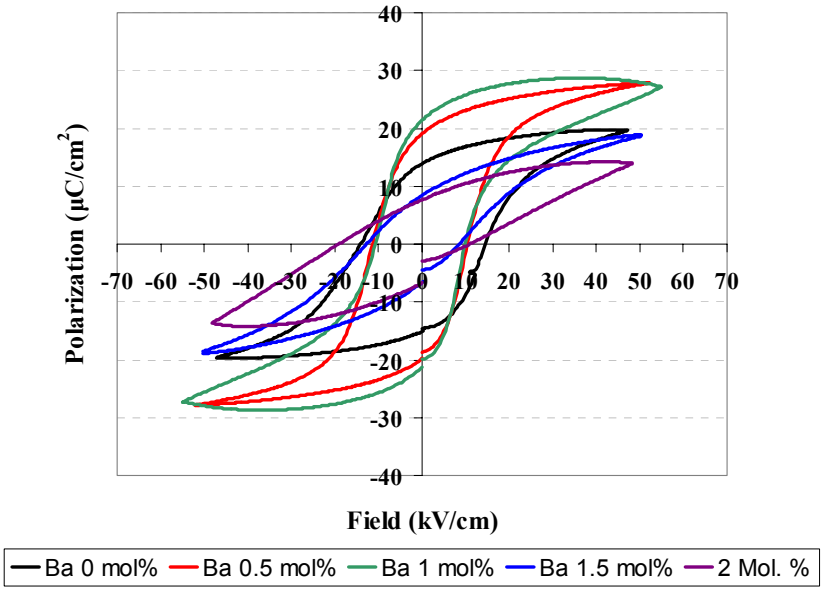

Fig. 4- The polarization-field behavior of samples with different molar percentages of Ba^{2+}.

Dielectric properties of the Ba^{2+} doped samples were studied within the temperature range of 75-350 ºC at 1 kHz. Shown in Fig. 5, the maximum dielectric constant for the base composition (0 mol.% Ba^{+2}) was 5500 with a curie temperature (T_c) of ~290 °C. For comparison, Saito had reported a curie temperature of 253 °C for the base composition. The observed 37 °C temperature difference could be due to the fact that (1) the base composition in this study was slightly different from that reported by Saito, (2) the base composition in our study has orthorhombic phase and Saito reported a tetragonal base at room temperature, (3) the base composition powder were prepared by two different methods. In this study we directly calcined a mixture of carbonate and oxide precursors to obtain final base composition while in Saito's work the calcined powder were prepared by mixing five precalcined binary systems (namely NN, KN, KT, LS, and NS). As the molar percentage of the Ba^{2+} increased, the T_c's shifted to lower temperatures and the corresponding maximum dielectric constants decreased. In addition, the widths of dielectric peaks were broadened with increasing the Ba^{2+} concentration. The notable permittivity decline when Ba^{+2} > 1 mol.% was attributed to the substantial change in the microstructure and crystalline phase of the samples, as discussed above and shown in Figures 2 and 3.

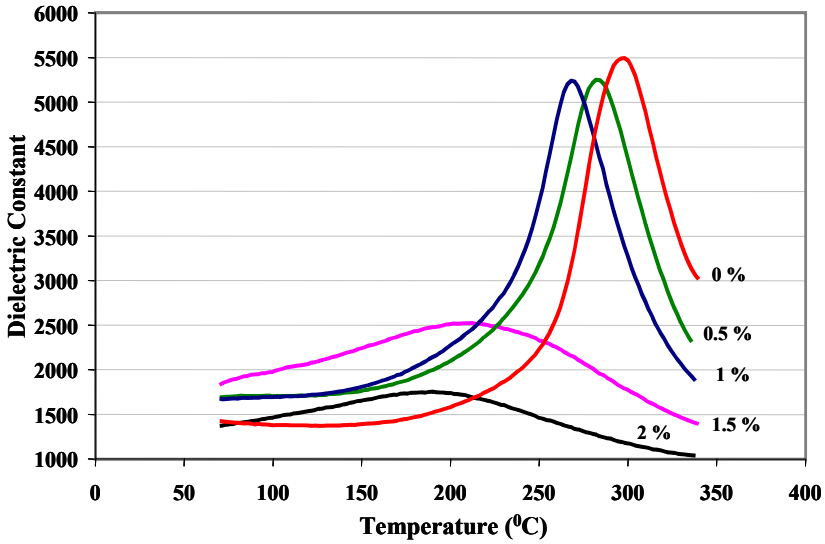

Fig. 5- The dielectric constant versus temperature for various Ba+2 concentration.

The room temperature permittivity and dielectric loss versus Ba^{+2} mol.% are depicted in Fig. 7. Samples had almost similar dielectric loss for Ba^{+2} content ≤ 1.5 mol.% and it abruptly increased to 5% for samples containing 2 mol.% Ba^{+2}. The dielectric constant of the samples increased and reached its maximum value at 1 mol.% and then decreased by further increase of Ba^{+2} content. This can be explained by the fact the addition of Ba^{+2} content ≥ 1.5 mol.% lowered the relative density of sintered bodies by reducing the grain size and trapping porosity in the microstructure. However, the substitution of various contents of the Ba^{+2} in A site significantly improved the room temperature dielectric permittivity.

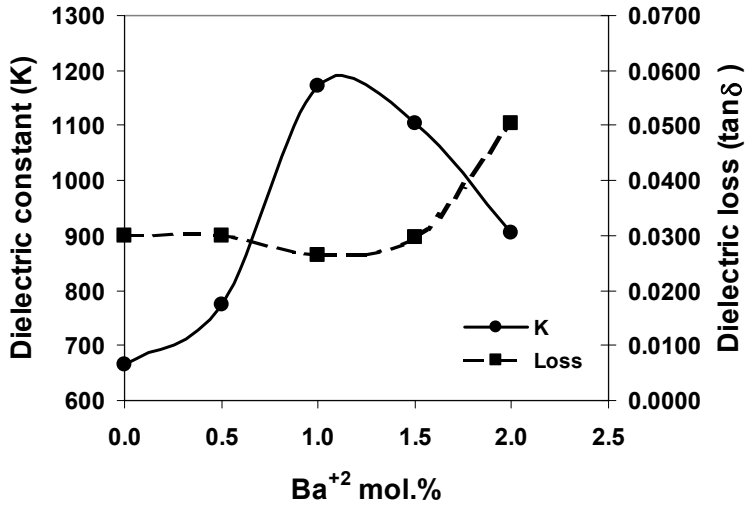

Fig. 6- The room temperature permittivity and dielectric loss versus Ba^{+2} mol.%.

Fig. 7 shows the piezoelectric properties (d_{33}, k_{33}, k_t, *and* k_p) of the samples versus the Ba^{+2} mol%. As seen, all piezoelectric properties represent similar trend, reaching to the maximum values at 1 mol%. Further increase of the Ba^{+2} concentration above 1 mol% gave rise to the reduction of all piezoelectric properties. It must be mentioned that above 1 mol%, the piezoelectric properties of the samples were even lower than those for the base composition with 0.0 mol% Ba^{+2}.

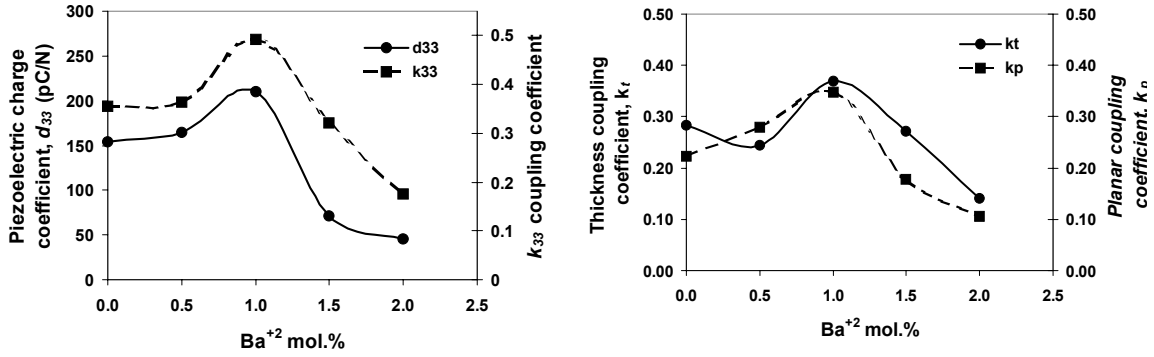

Fig. 7- The piezoelectric properties (d_{33}, k_{33}, k_t, *and* k_p) of the samples versus the Ba^{+2} mol.%.

To demonstrate the performance capability that can be achieved with the base composition, a single element ultrasonic transducer was fabricated. The probe had a single matching layer and air backing for maximum sensitivity. Fig. 8a schematically shows the structure of the transducer. The target was a stainless steel plate with dimension of 4x4x1 inches. The selected dimension was at least 10 times larger than wavelength of the ultrasonic sound. The ceramic disc was 10 mm in diameter and 0.85 mm thick. The front face of the ceramic was covered with silver past (7095, Dupont) to the edge while the electrode on the back face was 5mm in diameter located at the center of the ceramic disc. After firing the electrode at 500 °C for 5 minutes and poling, the ceramic disc was placed in epoxy housing and one wire of a coaxial cable was soldered to the back electrode. The ground wire of the coaxial cable was passed through an access orifice to the top surface and connected to the front electrode using silver epoxy (4922N, Dupont) cured at room temperature for 12 hours, as shown in Fig. 8a. An acoustic matching layer about 170 μm in thickness was bonded onto the front surface using ethyl cyanoacrylate (Elmer's Product Inc.). The sound velocity and acoustic impedance of the matching layer were 2460 m/s and 4.3 MRayls at 3.5 MHz, respectively. The complex electrical impedance of the probe was 58.0Ω with a capacitance of 614.387 pF. Fig. 8b shows a photograph of a fabricated ultrasonic probe.

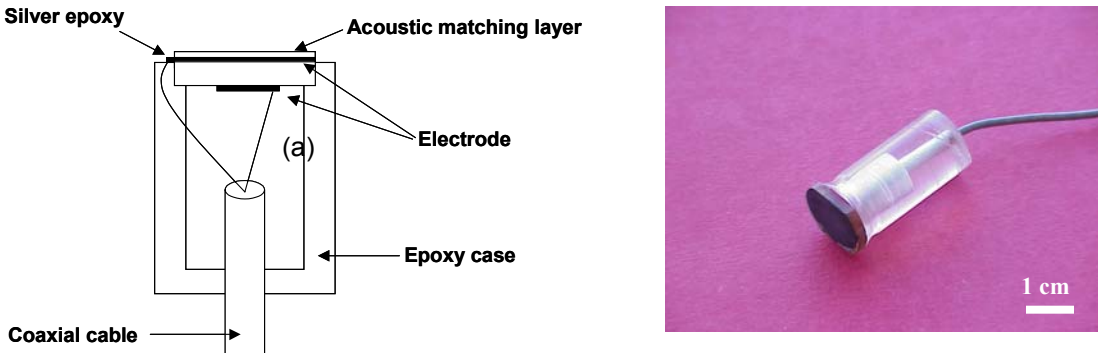

Fig. 8- (a) Schematic representation of the transducer probe (Left) and (b) photograph of a fabricated ultrasonic probe (Right).

Echo waveforms from a stainless steel plate were measured using a conventional pulse-echo method at room temperature. A standard pulser/receiver (Panametrics, Model 5800) was used with the following parameters: gain = 40 dB, energy level = 12.5 μJ, damping resistance = 25Ω. Fig. 9 shows measured pulse-echo characteristics of the probe. The center frequency, - 6dB fractional bandwidth, and insertion loss were 3.56 MHz, 36.8%, and –8.36 dB, respectively.

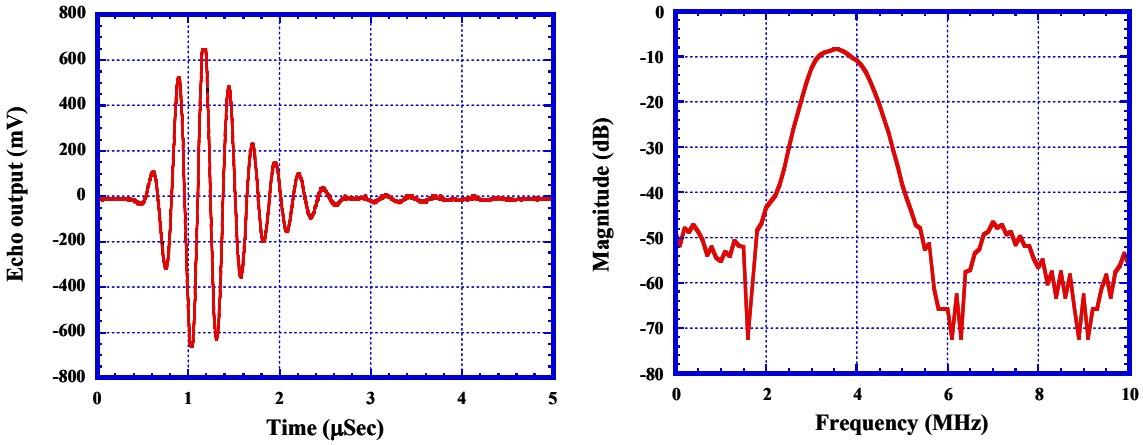

Fig. 9 Measured pulse-echo characteristics of the probe

SUMMARY AND CONCLUSION

Substitution of the Ba^{2+} as an A-site ion in the system of (Li,Na,K) (Nb,Ta,Sb)O_3 (KNN-LT-LS) with different molar percentages (0-2%) of Ba^{2+} was studied. The powders were pressed uniaxially and sintered at 1150 °C in oxygen atmosphere. The dielectric constant and all piezoelectric properties increased with the addition of up to 1 mol.% of Ba^{2+} and then decreased notably when the higher concentration of the Ba^{2+} was used. The Curie temperature shifted to lower temperatures by incorporation of Ba^{+2}. Room temperature permittivity is showing the increment by substitution of Ba^{2+} up to one mol.% while the maximum permittivity at T_c is shifted toward the lower temperatures. In the mean time, the shape of the permittivity-temperature peak is widening upon more Ba^{2+} substitution. Fabrication of a single air-backed probe transducer with KNN-LT-LS base composition realized a measured -6 dB fractional bandwidth of 36.8% and an insertion loss of –8.36 dB, at a center frequency of 3.56 MHz. Permittivity and piezoelectric properties along polarization and coercive results indicate the soft piezoelectric behavior when Ba^{2+} is substituted in the KNN-LT-LS system.

In conclusion, the importance of this system relative to other known lead-free piezoelectric ceramics are that (1) the piezoelectric and electromechanical properties are higher, (2) the biocompatibility is higher, thereby facilitating invasive/embedded medical ultrasound applications, and (3) the lower density results in a corresponding lower acoustic impedance, providing a more efficient match of acoustic energy into human tissue.

REFERENCES

[1] B. Jaffe, “Piezoelectric Ceramics”, *Academic Press*, pp. 214-217 (1971).

[2] J. M. Kelly, “A Study of Electromechanical Properties of PMN-PT Ceramics and Analysis of the Effects of Loss on Frequency Response of Piezoelectric Ceramics”, Rutgers University, Ph.D. Thesis (1998)

[3] Passmann C. and Em& H. 150 MHz in vivo ultrasound of the skin: imaging techniques and signal processing procedures, *IEEE Ultrasonics Symposium,* 1661-1664, 1994.

[4] Turnbull D. H., Starkoski B. G., Harasiewicz K. A., Semple I. L., From L., A.K. *G.,* Sauder D. N., and Foster F. S. A 40 -100 MHz B-scan ultrasound backscatter microscope far ski imaging., Ultra*sound in Medicine and Biology:21,* 79-88, 1995.

[5] Semple I. L., Gupta A. K., From L., Harasiewlcz K. A., assessment of high frequency (40-60 MHz) ultrasound Sauder D. N., Foster F. S., and Turnbull D. H. Preliminary imaging in the clinical assessment of cutaneous melanoma, *Anals ofplarticsurgery:34,599-@36,* 1995.
[6] M.J. Wiersema, C.R. Reilly. N.T. Sanghvi, R. Hawes. L. Wiersema and C. Aust, "Twenty-five *MHz* gastrointestinal ultrasonography," *IEEE* Ultrason. *Symp.Proc.,* pp 845-848, IEEE Cat. No. 89CH2791-2, EEE, New York, 1989.
[7] F.E. Silverstein, R.W. Martin, M.B. Kimmey, G.C. Jiranek, D.W. Franklin and A. Proctor, "Experimental evaluation of an endoscopic ultrasound probe: *In vitro*and *in vivo* canine studies," *Gastroenterology* vol. 96,pp. 1058-1062, 1989.
[8] Lockwoad G. R., Ryan L. K., Gotlleb A. I., Lonn E., Hunt I. W., Lui P., and Foster F. S. In vitro high resolution intravascular imaging in muscular and elastic arteries., *J. of* the *American Collegeo/Cordiology:20,* 153.160, 1992.
[9] Foster F. S., Knapik D. A., Machado J. C., Gallet I. M. C., Ryan L. K., and Nissen S. E. High frequency intracoronary ultrasound imaging, *Seminars in Interventional Cardiology,* In press, 1997.
[10] Christian Passmann and Helmut Ermert, "A 100-MHz Ultrasound Imaging System for Dermatologic and Ophthalmologic Diagnostics," IEEE TRANSACTIONS ON ULTRASONICS, FERROELECTRICS, AND FREQUENCY CONTROL, VOL. 43, NO. 4, JULY 1996
[11] Lukacs M., Sayer M., Knapik D., Candela R., and Foster F. S. Novel PZT films for Ultrasound Biomicroscopy, *IEEE Ultrasonics Symposium,* 1996.
[12] L.F. Brown, RL. Carlson and J.M. Sempsrott, "Spin-Cast P(VDF-TrFE) Films for High Performance Medical Ultrasound Transducers, "IEEE ULTRASONICS SYMPOSIUM – 1725-1727 (1997).
[13] Yokosawa K., Shinomura R., Sano S., Ita Y., Ishikawa S., and Sato Y. A 120 MHz probe for tissue imaging, *Ultrasonic* Imaging: l8,231-239, 1996.
[14] Zipparo M. I., Shung K. K., and Shrout T. R. Piezocerarnics for high frequency (20-100 MHz) single element imaging transducers, *IEEE Transaction on Ultrasonics, Ferroelectrics, and Frequency Control: 44,* 1038-1048, 1997.
[15] D.A. Knapik, B. Starkoski,, C.J. Pavlin and F.S. Foster, "A REALTIME 200 MHz *ULTRASOUND B-SCAN IMAGER,*" IEEE ULTRASONICS SYMPOSIUM, pp. 1457-1460, 1997.
[16] A. D. Corso, M. Posternak, R. Resta, and A. Baldereschi, *Phys. Rev. B*, **50** [15], pp. 10715 (1994).
[17] Yamada, H. Shimizo, and M. Minakata, *IEEE Ultrason. Sym. Proc.*, pp 745 (1986).
[18] H. Nagata, N. Chikoshi, T. Takenaka, "Ferroelectric Properties of Bismuth-Layered Structure Compound $Sr_xBi_{4-x}Ti_{3-x}Ta_xO_{12}$", *Jpn. J. Appl. Phy.,* 38, pp. 5497-5499 (1999).
[19] M. Suzuki, H. Nagata, J. Ohara, H. Funakubo and Takenaka, " $Bi_{3-x}M_xTiTaO_9$ (M=La or Nd) Ceramics with High Mechanical Quality Factor Q_m", *Jpn. J. Appl. Phys.*, 42, pp. 6090-6093 (2003).
[20] T. Sawada, A. Ando, Y. Sakabe, D. Damjanovic and N. Setter, "Properties of Elastic Anomaly in $SrBi_2Nb_2O_9$-Based Ceramics'' *Jpn. J. Appl. Phys.*, 42, pp. 6094-6098 (2003).
[21] C. Duran, S. Trolier-McKinstry, and G. L. Messing, "Fabrication and electrical properties of textured $Sr_{0.53}Ba_{0.47}Nb_2O_6$ ceramics by templated grain growth", *J. Am. Ceram. Soc.*, 83[9], pp. 2203-13 (2000).
[22] G. A. Smolenski, V. A. Isupov, A. I. Agranovskaya, and N. N. Krainik, "New Ferroelectrics of Complex Composition IV", *Sov.. Phys. Solid State*, 2[11], pp. 2651-54 (1961).
[23] H. Nagata, M. Yoshida, Y. Makiuchi, and T. Takenaka, "Large Piezoelectric Constant and High Curie Temperature of Lead-free Piezoelectric Ceramic Ternary System Based on Bismuth Sodium Titanate-Bismuth Potassium Titanate-Barium Titanate near the Morphotropic Phase Boundary", *Jpn. J. Appl. Phy*., 42, No. 12, pp. 7401-7403 (2003).
[24] L. Egerton, D.M. Dillon, "Piezoelectric and Dielectric properties of the Ceramics in the system Potassium-Sodium Niobate'', *J. Am. Ceram. Soc.*, 42, pp 438-442 (1959).
[25] G. Shirane, R. Newnham, R. Pepinsky, "Dielectric Properties and Phase transitions of $NaNbO_3$ and $(Na,K)NbO_3$", *Phys. Rev*. 96, pp. 581-588 (1954)
[26] G. H. Haertling, *J. Am. Ceram. Soc*., 50, pp. 329 (1967).
[27] R. E. Jaeger, L. Egerton, "Hot pressing of Potassium-Sodium Niobates", *J. Am. Ceram. Soc*., 45, pp. 209-213 (1962).

[28] L. E. Cross," Electric double hysteresis in $(K_xNa_{1-x})NbO_3$ single crystals", *Nature*, 181, pp. 178-179 (1958).
[29] M. Kosec and D. Kolar, "On Activated Sintering and Electrical Properties of $KNaNbO_3$", *Mater. Res. Bull.*, 10, pp. 335-340, (1975).
[30] H. Birol, D. Damjanovic, and N. Setter, "Preparation and Characterization of $(K_{0.5}Na_{0.5})NbO_3$ Ceramics", *J. Eur. Ceram. Soc.*, In Press (2005).
[31] S. Z. Ahn and W. A. Schulze, "Conventionally Sintered $(K_{0.5}Na_{0.5})NbO_3$ with Barium Additions", *Commun. Am. Ceram. Soc.*, 70, C18-C21 (1987).
[32] V. Bobnar, B. Malic, J. Holc, and M. Kosec, "Electrostrictive Effect in Lead-free Relaxor $K_{0.5}Na_{0.5}NabO_3$-$SrTiO_3$ Ceramic System", *J. Appl. Phy.*, 98, (2005)
[33] M. Matsubara, T. Yamaguchi, K. Kikuta, and S. Hirano, "Sinterability and Piezoelectric Properties of (K,Na)NbO_3 Ceramics with Novel Sintering Aid", 43, No.10, pp.7159-7163 (2004).
[34] M. Matsubara, T. Yamaguchi, K. Kikuta, and S. Hirano, "Sintering and Piezoelectric Properties of Potassium-Sodium Niobate Ceramics with Newly Developed Sintering Aid", *Jpn. J. Appl. Phy.,* 44, No.1A, pp.258-263 (2005)
[35] M. Matsubara, K. Kikuta, and S. Hirano," Piezoelectric Properties of $(K_{0.5}Na_{0.5})(Nb_{1-x}Ta_x)O_3$-$K_{5.4}Cu_{1.3}Ta_{10}O_{29}$ Ceramics", 97, *J. Appl. Phy.*, (2005)
[36] M. Matsubara, T. Yamaguchi, K. Kikuta, and S. Hirano, "Effect of Li^+ Substitution on the Piezoelectric Properties of Potassium Sodium Niobate Ceramics", *Jpn. J. Appl. Phy.*, 44, No. 8, pp. 6136-6142 (2005)
[37] S-H. Park, C-W. A, S. Nahm, and J-S. Song, "Microstructure and Piezoelectric Properties of ZnO-Added $(Na_{0.5}K_{0.5})NbO_3$ Ceramics", *Jpn. J. Appl. Phy.*, 43, No. 8B, pp. L1072-L1074 (2004).
[38] Y. Guo, Ken-ichi Kakimoto, H. Ohasto, "$(K_{0.5}Na_{0.5})NbO_3$-$LiTaO_3$ Lead-free Piezoelectric Ceramics", *Matt. Lett.*, 59, pp. 241-244, (2005).
[39] Y. Saito, H. Takao, T. Tani, T. Nanoyama, K. Takatori, T. Homma, T. Nagaya, and M. Nakamura, "Lead-free Piezoceramics", *Nature*, 123, pp. 84-87 (2004)
[40] The Institute of Electrical and Electronics Engineers (IEEE), Standards on Piezoelectricity, *American National Standards Institute,* ANSI/IEEE Std 176, 1987.
[41] F. A. Kroeger, "Chemistry of Imperfect Crystals", North-Holland, Amesterdam, The Netherlands, 1964.
[42] M. Takahashi, "Electrical Resistivity of Lead Zirconate Titanate Ceramics Containing Impurites", *Jpn. J. Appl. Phy.*, vol. 10, 5, pp 643-650 (1971)
[43] E. Furman, W. Gu, and L. E. Cross, " Electrical Properties of PLZT 9.5/65/35 Ceramics", *IEEE/UFFC Proceedings*, pp. 588-590 (1991)
[44] R. Gerson and H. Jaffe, "Electrical Conductivity in Lead Titanate Zirconate Ceramics", *J. Phys. Chem. Solids*, vol. 24, pp. 979-984 (1963)
[45] J. J. Dih and R. M. Fulrath,"Electrical Conductivity in Lead Zirconate-Titanate Ceramics", *J. Am. Ceram. Soc.*, vol. 61, pp. 448-451 (1978)
[46] G. Haertling," Ferroelectric Ceramics: History and Technology", *J. Am. Ceram. Soc.*, Vol. 82, No. 4, (1999).
[47] T. Takenaka, "Grain Orientation Effects on Electrical Properties of Bismuth layer-Structure Feroelectric Ceramics, *J. Ceram. Soc. Jpn.*, 110 [4] pp. 215-224,(2002).
[48] Y. Saito and H. Takao, "Nb-Perovskite Structured Piezoelectric Ceramics for Sensors and Actuators", *The Twelfth US-Japan Seminar on Dielectric and Piezoelectric Ceramics*, November 6-9, (2005).
[49] T.R.Shrout, R. Eitel, C. Randall, "High performance, high temperature perovskite piezoelectric ceramics", *Piezoelectric Materials in Devices, Extensive Reviews on Current and Emerging Piezoelectric Materials, Technology, and Applications*, Ed. by Neva Setter, Ceramics Laboratory, EPFL, 2002